ELSEVIER

Biophysical Chemistry 86 (2000) 191–201

Biophysical Chemistry

www.elsevier.nl/locate/bpc

Intermolecular dynamics and function in actin filaments ☆

Eldar Kim, Emil Reisler*

Department of Chemistry and Biochemistry and the Molecular Biology Institute, University of California, Los Angeles, CA 90095, USA

Received 20 January 2000; received in revised form 16 March 2000; accepted 16 March 2000

Abstract

Structural models of F-actin suggest that three segments in actin, the DNase I binding loop (residues 38–52), the hydrophobic plug (residues 262–274) and the C-terminus, contribute to the formation of an intermolecular interface between three monomers in F-actin. To test these predictions and also to assess the dynamic properties of intermolecular contacts in F-actin, Cys-374 pyrene-labeled skeletal α-actin and pyrene-labeled yeast actin mutants, with Gln-41 or Ser-265 replaced with cysteine, were used in fluorescence experiments. Large differences in Cys-374 pyrene fluorescence among copolymers of subtilisin-cleaved (between Met-47 and Gly-48) and uncleaved α-actin showed both intra- and intermolecular interactions between the C-terminus and loop 38–52 in F-actin. Excimer band formation due to intermolecular stacking of pyrene probes attached to Cys-41 and Cys-265, and Cys-41 and Cys-374, in mutant yeast F-actin confirmed the proximity of these residues on the paired sites (to within 18 Å) in accordance with the models of F-actin structure. The dynamic properties of the intermolecular interface in F-actin formed by loop 38–52, plug 262–274 and the C-terminus may account for the observed cross-linking of these sites with reagents < 18 Å. The functional importance of actin filament dynamics was demonstrated by the inhibition of the in vitro motility in the Gln-41–Cys-374 cross-linked actin filaments.

Keywords: Actin filaments; Intermolecular interface; Intermolecular dynamics; Pyrene fluorescence; Excimer fluorescence; Cross-linking

Abbreviations: ANP, *N*-(4-azido-2-nitrophenyl) putrescine; G-actin, monomeric actin; F-actin, filamentous (polymerized) actin; Q41C actin, yeast actin with Gln-41 mutated to cysteine; Q41C/C374S actin, yeast actin with Gln-41 mutated to cysteine and Cys-374 replaced with serine; S265C/C374A actin, yeast actin with Ser-265 mutated to cysteine and Cys-374 replaced with alanine

☆ Dedicated to Heini Eisenberg.

* Corresponding author. Tel.: +1-310-825-3531; fax: +1-310-206-8010.

E-mail address: reisler@mbi.ucla.edu (E. Reisler).

0301-4622/00/$ - see front matter
PII: S0301-4622(00)00143-5

1. Introduction

It is a privilege to contribute to this issue of *Biophysical Chemistry*, dedicated to honoring the contributions of Heini Eisenberg to the biophysical and biopolymer science, and to pay tribute to him as a scientist, mentor and a friend. Thirty years ago Heini Eisenberg returned to the Weizmann Institute of Science from a sabbatical year at NIH infected by Gordon M. Tomkins with an enthusiasm for and great interest in protein self-assembly systems and their structure–function relationships. One of us (E.R.), as a graduate student, was fortunate to have been introduced into this area and inspired by Heini Eisenberg. Today, even more than then, studies on the assembly and function of organized protein structures are central to the understanding of many biological processes. The actin filaments are a prime example of the need to link diverse cellular functions to the structure and dynamics of a large oligomeric system.

The prevailing model of F-actin filaments structure [1] and the refined versions of this model [2,3] are based on fitting the atomic structure of monomeric (G-) actin (complexed to DNase I) to X-ray fiber diffraction data of oriented actin gels of approximately 8 Å resolution. Although this model is consistent with a large body of biochemical and structural data, there are many observations which reveal that actin filaments can exist in different conformational states. For example, it has been noted long ago that F-actin exhibits natural variations in its helical twist [4] and that some actin binding proteins (e.g. cofilin) change the mean twist per subunit to a substantial degree [5]. Orlova and Egelman [6–8] found that F-actin can equilibrate between at least two conformational states distinguished by the orientations of subdomain 2 and the positions of the C-terminus, depending on the divalent cation and/or nucleotide bound to actin. The importance of subdomain 2, and in particular its DNase I binding loop (residues 38–52), to F-actin structure and function was demonstrated in several biochemical studies [9–11] leading to speculations that the motions of subdomain 2 in F-actin are involved in its regulation by tropomyosin and troponin [12]. In parallel, it has been also recognized that modifications of actin's C-terminus affect the structural and functional properties of F-actin [8,13–16]. Moreover, spectroscopic [17] and proteolytic digestion [16] experiments showed that the above two structural elements (loop 38–52 and the C-terminus) appear to be intramolecularly coupled to each other despite their significant separation on G-actin.

The interest in the potential intermolecular coupling of the C-terminus and the loop 38–52 on actin [18] is stimulated by the functional implications of such a coupling. The evidence for long range cooperativity in F-actin, as revealed in structural studies on gelsolin [19] and myosin subfragment 1 (S1) binding to actin [20], has been linked to the propagation of structural changes in F-actin through intermolecular contacts, which most likely involve the subdomain 2 region. Structural studies suggested also that loop 38–52, the C-terminus, and the hydrophobic plug (residues 262–274) which stabilizes the interstrand interactions in F-actin [1] interact to form an intermolecular interface in F-actin [3,21]. However, model-derived [2] distances (~ 20 Å) between key residues (Q41, S265, C374) at these structural elements appear to be beyond the range that would allow for a direct contact between them. Such interactions, if present, may result from dynamic properties of the intermolecular interface in F-actin.

In this study we explored the intermolecular interface in F-actin and the interactions of loop 38–52, plug 262–274, and C-terminus with each other by using yeast actin mutants with cysteine substitutions in these structural elements. We show by pyrene fluorescence, excimer fluorescence and cross-linking experiments both the dynamic nature of these sites and the importance of structural flexibility at the intermolecular interface in F-actin to its biological functions in motion generation with myosin.

2. Materials and methods

2.1. Reagents

The QuikChange™ site directed mutagenesis kit, DNA restriction enzymes, and plasmid pur-

ification kit were purchased from Stratagene (La Jolla, CA), New England Biolabs (Beverly, MA) and Qiagen (Valencia, CA), respectively. Peptone, tryptone and yeast extract were from Difco (Detroit, MI). DNase I was purchased from Worthington Biochemical Corporation (Lakewood, NJ). Pyrene maleimide and rhodamine phalloidin were from Molecular Probes (Eugene, OR). Subtilisin, dibromobimane, ATP, DTE and phalloidin were obtained from Sigma Chemical Company (St. Louis, MO). Bacterial transglutaminase was a gift from Drs Masao Motoki and Katsuya Seguro.

2.2. Oligonucleotide-directed mutagenesis

Actin mutagenesis was performed according to the Stratagene (La Jolla, CA) QuikChange procedure using oligonucleotides purchased from Genset Corp. (San Diego, CA). Double-stranded yeast shuttle plasmid pTD24 [22] which carries a copy of the ACT1 gene was used as a template for mutagenesis. Oligonucleotide primers 5′-CAAGACACtgtGGTATCATGGTCGG-3′ and 5′-CCGAACCATGATACCacaGTGTCTTGG-3′ were used to introduce the Q41C actin mutation, and the primers, 5′-CAGAGATTAGAAgcttTTGTGGTGAAC-3′ and 5′-GTTCACCACAAaagcTTCTAATCTCTG-3′ were used to generate the C374S actin mutation. The mutated sequences are shown in lowercase and selective restriction enzyme markers are underlined. The *Sty*I site is lost in Q41C and the *Hin*dIII site is added in C374S. Actin genes from screened plasmid clones were sequenced (GeneMed, San Francisco, CA) to confirm the absence of random errors.

2.3. Yeast transformation

Mutant plasmids carrying HIS3 marker were transformed into the diploid yeast strain TDS101 [22], which has a single ACT1 gene copy on the plasmid with URA3 marker and genomic copies of ACT1 gene deleted. The original plasmid carrying ACT1 gene was sorted out by plasmid shuffling [23]. The cells were screened for HIS^+ and URA^- phenotype, which resulted in yeast cells carrying a homozygous copy of mutant actin gene.

2.4. Preparation of actin

Skeletal α-actin was isolated from an acetone powder of rabbit muscle according to the procedure of Spudich and Watt [24]. Actin was cleaved with subtilisin as reported by Schwyter et al. [25]. SDS-PAGE analysis of actin revealed almost complete (between 90 and 100%) cleavage of actin into the 35 and 9 kDa fragments [25]. Yeast actin was purified from yeast cells by affinity chromatography on DNase I column as described previously [26]. Prior to its elution, the column-bound actin was washed with 1.0 M NaCl in G-actin buffer (10 mM Tris–HCl at pH 7.8, 0.2 mM ATP, 0.2 mM β-mercaptoethanol, and 0.2 mM $CaCl_2$) to remove cofilin [27]. All actin solutions were polymerized by the addition of 3.0 mM $MgCl_2$ and stoichiometric amounts of phalloidin.

2.5. Fluorescence measurements

Skeletal α-actin and yeast actin were labeled with pyrene maleimide as reported before [28]. The extent of actin labeling was determined as in that study [28]. Fluorescence spectra of pyrene-labeled actin were recorded in a Spex Fluorolog spectrofluorometer (Spex Industries, Inc., Edison, NJ) at 25°C.

2.6. Cross-linking of F-actin by N-(4-azido-2-nitrophenyl) putrescine (ANP)

Transglutaminase mediated cross-linking of Gln-41 to Cys-374 in F-actin by ANP was carried out as described by Hegyi et al. [29]. The percentage of actin cross-linking was determined by monitoring the amount of uncross-linked actin monomer on SDS-PAGE.

3. Results

3.1. Intermolecular and intramolecular coupling between loop 38–52 and the C-terminus

Fluorescence changes of a pyrene probe attached to Cys-374 on actin provide a sensitive test

for conformational transitions at the C-terminus which are associated with the polymerization of G-actin to F-actin and S1 binding [30]. For this reason, pyrene modified skeletal α-actin was used to assess the inter- and intramolecular coupling between the C-terminus and loop 38–52 on actin. The loop was specifically cleaved by subtilisin between Met-47 and Gly-48 [25], both on labeled and unlabeled actin. Emission spectra of actin polymers and copolymers of cleaved and uncleaved actin are shown in Fig. 1. As observed earlier [10], pyrene fluorescence is much smaller in the cleaved (curve D) than in the intact (curve A) F-actin. The large difference in the fluorescence of these F-actins is not caused by different extents of actin assembly since the presence of phalloidin drives the polymerization reaction to completion in all samples.

Cleavage-induced changes in both intra- and intermolecular interactions in F-actin can be evoked to explain the different fluorescence of cleaved and uncleaved F-actin. Intramolecular coupling between loop 38–52 and the C-terminus was deduced from cleavage-related changes in the energy transfer between actin tryptophans in subdomain1 and AEDANS attached to Cys-374 [17]. Intermolecular coupling between the DNase I binding loop and the C-terminus was established via quenching in F-actin of a dansyl probe attached to Gln-41 by Cu^{2+} bound to Cys-374 [18]. The copolymers of cleaved and uncleaved actin used in the experiments shown in Fig. 1 enabled the assessment of these two modes of conformational perturbation of the C-terminus using the same experimental system. When 1.0 μM subtilisin cleaved pyrenyl actin was copolymerized with 7.0 μM unlabeled G-actin, either uncleaved (spectrum C in Fig. 1) or cleaved (spectrum D in Fig. 1), the fluorescence intensities in the corresponding spectra differed by a factor of 1.5 (at $\lambda_{max} = 405$ nm). The main difference between the polymers used in spectra C and D is in the intermolecular contacts formed by the C-terminus region of pyrenyl actin with the cleaved and uncleaved actins. The same argument applies also to the comparison of spectra B and A in Fig. 1, which correspond to 1.0 μM uncleaved pyrenyl actin copolymerized with 7.0 μM unlabeled actin, cleaved and uncleaved, respectively. These two sets of emission spectra (A and B, C and D) confirm the intermolecular coupling between the C-terminus and loop 38–52 in F-actin [18].

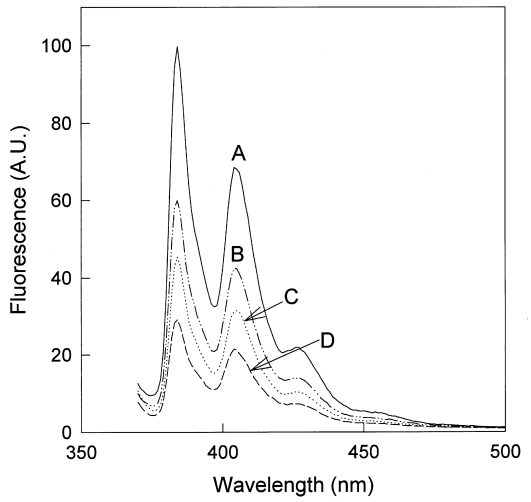

Fig. 1. Emission spectra of Cys-374 pyrene-labeled F-actin. All actin solutions contained 1.0 μM pyrene-labeled α-actin, either intact (spectra A and B) or subtilisin cleaved (spectra C and D), and 7.0 μM unlabeled actin, either intact (spectra A and C) or subtilisin cleaved (spectra B and D). The actin mixtures were polymerized with 3.0 μM $MgCl_2$, and stoichiometric amounts of phalloidin. Pyrene labeling and subtilisin cleavage of actin were carried out as described in Section 2. The excitation wavelength was set at 365 nm.

The intramolecular coupling between loop 38–52 and the C-terminus is evident from the comparison of spectra B and D or A and C in Fig. 1. These spectra correspond to copolymers formed using the same main component (7.0 μM cleaved actin for B and D and 7.0 μM intact actin for A and C) but different pyrene labeled actins, cleaved or uncleaved. In these polymers, the C-terminal region in the cleaved and uncleaved pyrenyl actins is likely to have the same intermolecular contacts with the main actin component (the 7.0 μM actin) of the polymer. Thus, the two-fold difference in the fluorescence intensities of spectra B and D, and A and C attests to intramolecular coupling between loop 38–52 and the C-terminus. Clearly, the difference in the intermolecular contacts made by loop 38–52 in the cleaved and uncleaved

pyrenyl actin is sensed by the C-terminal pyrene probe. Thus, the pyrene fluorescence experiments shown in Fig. 1 confirm both the intra- and intermolecular coupling of the DNase I binding loop and the C-terminus in F-actin.

3.2. Excimer fluorescence of yeast actin mutants as a probe of intermolecular interface

To probe more directly the intermolecular interactions of loop 38–52 with the C-terminus and the hydrophobic plug (residues 262–274) in actin, we prepared new yeast actin mutants Q41C (with Gln-41 replaced with cysteine) and Q41C/C374S (with both Gln-41 and Cys-374 mutations), and also used the mutant S265C/C374A described in our previous study [28]. The choice of Gln-41 in loop 38–52 for cysteine substitution was influenced by the earlier observation of intermolecular coupling between a fluorescent probe attached to this residue and the Cu^{2+} bound to Cys-374 [18]. However, the mechanism of such coupling remains unclear since the adjacent Gln-41 and Cys-374 residues are ~ 23 Å apart (Fig. 2) in the Lorenz et al. [2] model of F-actin structure.

Cys-41 and Cys-265 in mutant actins are reactive and readily labeled with pyrene maleimide resulting in proteins with 2:1 (Q41C actin, with Cys-41 and Cys-374 labeled) and 1:1 (for Q41C/C374S and S265C/C374A) molar ratios of pyrene to actin. The excitation spectra of pyrene labeled Q41C, Q41C/C374S, and S265C/C374A actins are shown in Fig. 3. All three spectra are similar to each other and to the excitation spectrum of Cys-374 pyrene labeled actin [30]. Two noticeable aspects of Fig. 3 are the small red shift of the Q41C actin spectrum ($\lambda_{max} = 343$ nm) compared to those of the other two actins ($\lambda_{max} = 340$ nm), and the relatively low quantum yield of Q41C actin, which has two pyrene probes

Fig. 2. Wire representation of three actin monomers in the Lorenz et al. [2] model of F-actin structure. Monomers 1 and 3 are the adjacent actins within the same strand in F-actin. Residues Q41 (top) and C374 (bottom) in monomer 1 are identified by lightly shaded balls and are 47 Å apart from each other. S265 on monomer 2 is shown with gray balls and C374 on monomer 3 is identified by dark balls. The model-derived intermolecular distances between the pairs Q41-C374, Q41-S265, and S265-C374 are shown on the schematic and enlarged, triangle representation of the arrangement of these residues at the molecular interface of monomers 1, 2 and 3 in F-actin.

attached to it. Both the red shift and the decreased quantum yield of pyrene probes in Q41C actin indicate their exposure to a more polar environment than that of single probes attached to Cys-41 and Cys-265. The emission spectra of pyrene labeled Q41C/C374S and S265C/C374A are shown in Fig. 4 a,b, respectively). The polymerization of Q41C/C374S G-actin to F-actin leads to an approximately 30% increase in pyrene fluorescence (at $\lambda = 385$ nm) (Fig. 4a); the polymerization of S265C/C374A G-actin enhances its fluorescence only by approximately 7% (Fig. 4b). As expected, the emission spectra of these F-actins, which contain only one pyrene probe per actin, do not reveal the presence of an excimer band. However, a copolymer (1:1 mixture) of these two single labeled pyrene yeast actins, but not their monomeric mixture, shows an excimer band in the emission spectrum, with λ_{max} at 470 nm (Fig. 5a). This excimer reports on the spatial proximity (between 3.0 and 18 Å) of the Cys-41 and Cys-265 residues on Q41C/C374S and S265C/C374A actins in the copolymer. Clearly, the probability for such stacking arrangement of pyrene probes attached to Cys-41 and Cys-265 would be increased if a double-labeled yeast actin mutant (Q41C/S265C/C374S) could be prepared.

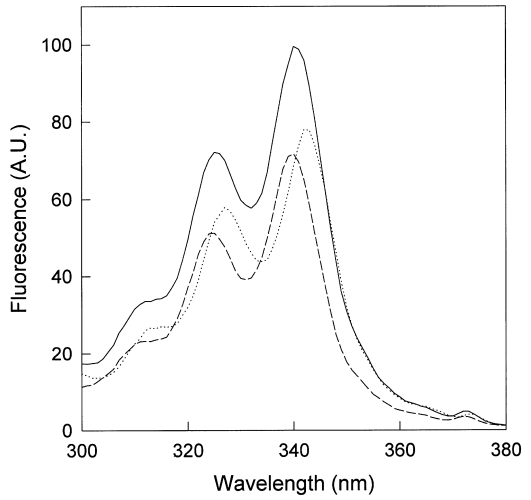

Fig. 3. Excitation spectra of pyrene labeled yeast F-actins. The spectra were recorded on 4.0 μM solutions of Q41C/C374S (—), S265C/C374A (---), and Q41C (· · ·) yeast actin mutants. Pyrene labeling stoichiometries were 1:1 and 2:1 pyrenes per actin for the first two and the third actin mutant, respectively. The emission wavelength was set at 393 nm. Fluorescence intensities are reported in arbitrary units (AU).

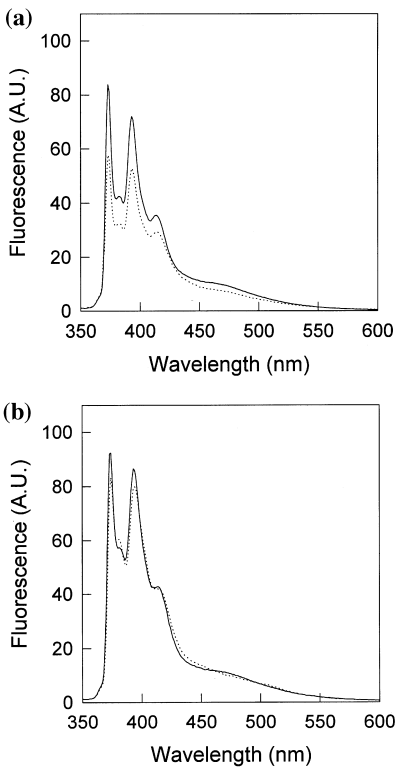

Fig. 4. Emission spectra of pyrene-labeled Q41C/C374S and S265C/C374A yeast actins. The spectra of G-actin (· · ·) and F-actin (—) were recorded on solutions of 4.0 μM pyrene-labeled actin (1:1 molar ratio pyrene/actin). (a) Q41C/C374S actin; (b) S265C/C374A actin. The excitation wavelength was set at 340 nm. Fluorescence intensities are given in arbitrary units (AU).

The emission spectra of the G- and F-actin forms of the Q41C double-labeled mutant actin are shown in Fig. 5b. The spectrum of G-actin is similar to that of the other (single) pyrene labeled actin mutants (Fig. 5a). The polymerization of pyrene-labeled Q41C yeast actin results in approximately 35% decrease in the monomer pyrene fluorescence (at $\lambda = 385$ nm) and the formation

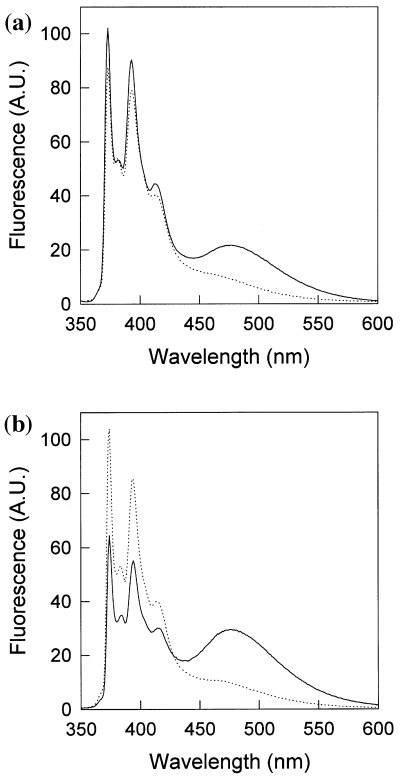

Fig. 5. Emission spectra of pyrene-labeled yeast actin mutants. (a) Mixture (1:1) of Q41C/C374S and S265C/C374A actins; (b) Q41C actin. The spectra in a and b were recorded at total actin concentrations of 4.0 μM G-actin (· · ·) and after the polymerization of these actins to F-actin (—). The excitation wavelength was set at 343 nm.

of a strong excimer band. The quenching of monomer pyrene fluorescence upon polymerization of Q41C actin is somewhat unexpected since the fluorescence of actins with single pyrene probes attached to Cys-41 (Fig. 4a), and especially to Cys-374 [30], increases upon their G to F transition. To a large extent, the quenching of monomer pyrene fluorescence in Q41C F-actin may be due to the excimer formation, but local changes in the environment of the pyrene probes due to their stacking cannot be ruled out. As above, the presence of pyrene excimer band in the Q41C F-actin shows the proximity to within 18 Å of Cys-41 and Cys-374 residues on adjacent actin monomers in F-actin.

3.3. Dynamic properties of the intermolecular interface in F-actin and filament function

The stacking of pyrene maleimide probes attached to Cys-41 and Cys-374, and Cys-265 and Cys-41 in mutant F-actins, which yields the excimer bands shown in Fig. 5, constrains the distance between these pairs of residues in actin filaments to between 3 and 18 Å [31]. At the higher end, this constrain is consistent with the distances between the above residues in the Lorenz et al. [2] model of F-actin structure (Fig. 2). The possibility that the excimer bands reflect a closer arrangement of the probed residues in F-actin is supported by the results of our cross-linking experiments. We have shown recently that a photoactivated reagent, *N*-(4-azido-2-nitrophenyl) putrescine, which is attached to Gln-41 in α-actin via a transglutaminase reaction, cross-links Gln-41 to Cys-374 on adjacent monomers in F-actin [29]. This cross-linking reaction leads to the formation of cross-linked dimers, trimers and higher order actin oligomers, which can be visualized on SDS-PAGE (Fig. 6). The cross-linking span of the reagent, between 11.1 and 12.5Å [29], suggests that the cross-linked residues can approach each other to at least that distance. Moreover, disulfide cross-linking experiments carried out on the Q41C yeast F-actin and the Q41C/C374S and S265C/C374A copolymers revealed that disulfide bonds are readily formed between these cysteines under oxidizing conditions (Kim et al., in press). These results provide evidence for dynamic properties of the three structural elements examined in this study (loop 38–52, plug 262–274 and the C-terminus) and for their direct interactions to form and/or stabilize the intermolecular interface in F-actin.

The question of the possible functional role for flexibility and dynamic transitions at the intermolecular interface in F-actin (loop 38–52/plug 262–274/C-terminus) was addressed by monitoring the motion of actin filaments over myosin in the in vitro motility assays. As shown in Fig. 6, the cross-linking of Gln-41 to Cys-374 inhibits the speed of filament motion and abolishes it completely at higher extents of cross-linking. Actin filaments in which all monomers are cross-linked

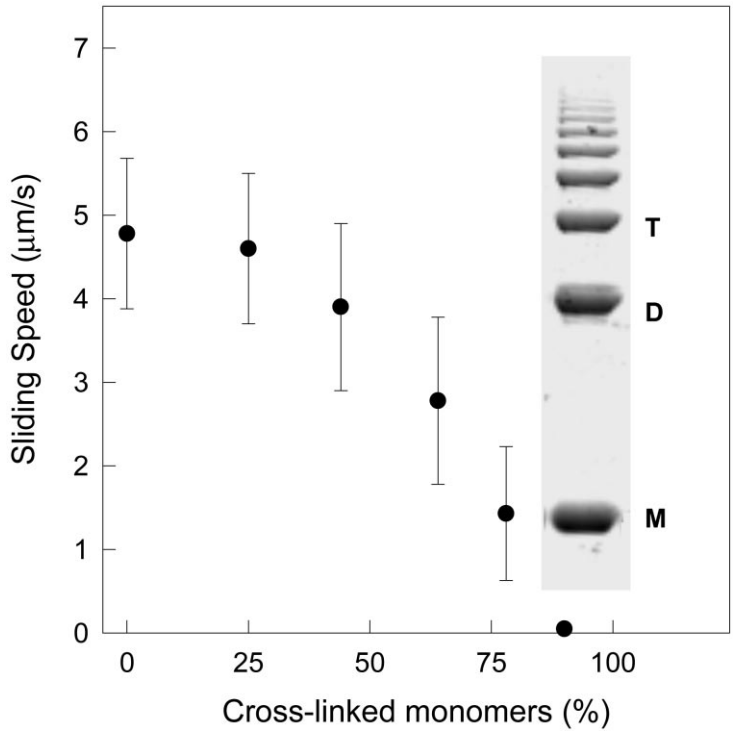

Fig. 6. In vitro motility and SDS-PAGE pattern of ANP cross-linked α-actin filaments. ANP [*N*-(4-azido-2-nitrophenyl) putrescine] cross-linking of skeletal α-actin filaments and the in vitro motility assays of actin were carried out as previously described [29,32]. The percentage of cross-linked actin in each sample was determined by SDS-PAGE analysis of the remaining uncross-linked actin monomer (denoted by letter M next to the protein band in the SDS-PAGE lane). The extent of F-actin cross-linking was controlled as before [29], by changing the ratio of ANP-Q41-labeled to unlabeled actin in the G-actin mixture prior to its polymerization and UV photocross-linking. The sliding speeds of between 100 and 200 actin filaments were determined under standard conditions [22] in each of the in vitro motility assays (at 25°C). Filament motion was analyzed using the motion analysis system (Santa Rosa, CA). The SDS-PAGE lane shows the distribution of cross-linked actin species, including monomers (M), dimers (D), trimers (T) and higher order oligomers following the ANP cross-linking of 70% of actin monomers.

into dimers, trimers and higher order oligomers do not generate motion with myosin (Fig. 6). However, such filaments are not greatly impaired in other aspects of actomyosin interactions namely, myosin binding and the activation of myosin ATPase activity [32]. Also, ANP-labeled but uncross-linked actin filaments move at the same speeds over myosin as unlabeled filaments.

This leads to the conclusion that the dynamic changes that occur at the uncross-linked intermolecular interface examined in this study are an essential element of the mechanochemical coupling and motion generation in actomyosin.

4. Discussion

The goal of this work has been to test for possible direct interactions of the DNase I binding loop, the hydrophobic plug and the C-terminus at the interface formed by three adjacent monomers in F-actin. Such interactions were predicted in the existing models of F-actin structure [1–3], and then proposed on the basis of interpretation of electron microscopy images of actin filament [21], but were not verified in direct experiments. Biochemical evidence also suggested a link between the above structural elements in

actin by showing that their modifications altered the polymerization and the actomyosin function of actin. Thus, for example, the subtilisin cleavage of loop 38–52 inhibits the in vitro motility of actin filaments [9], as do also some modifications of Cys-374 on actin [8,16].

Fluorescence evidence presented in this work for both intra- and intermolecular coupling between loop 38–52 and the pyrene labeled C-terminus region provides a simple explanation for the previous observations of functional perturbation of actin through the manipulation of each one of these sites. Yet, the above couplings did not establish a direct interaction between the 38–52 loop and the C-terminus on actin. Such a goal was pursued with the help of yeast actin mutants with cysteine residues introduced at residues 41 and 265. The Q41C yeast actin mutant enabled the attachment of two pyrene molecules to actin, at Cys-41 and Cys-374. This, in turn, led to the formation of a pyrene excimer band in the emission spectrum of the labeled actin, a clear indication that Cys-41 and Cys-374 on adjacent actin monomers in F-actin (monomers 1 and 3 in Fig. 2) must approach each other to within at least 18 Å. Strikingly, a similar conclusion about the proximity of Cys-41 and Cys-265 (on monomers 1 and 2 in Fig. 2) was reached on the basis of an excimer band in copolymers of pyrene-labeled Q41C/C374S and S265C/C374A.

As the condition for excimer formation (the stacking of pyrene rings) can be satisfied over a range of cysteine-to-cysteine distances (3–18 Å), depending on the local geometry of sites, orientation of cysteine residues, and the length of the probe linker, additional distance constrains were obtained from cross-linking experiments. The cross-linking of Gln-41 to Cys-374 on actin with an $\sim$11 Å long reagent (ANP), and disulfide bridging of Cys-41 to Cys-374 and Cys-41 to Cys-265 in yeast actin mutants (unpublished), show that the distance between these residues is not fixed in F-actin. Together with the pyrene excimer results, these data demonstrate the dynamic nature of the intermolecular interface created by the above three sites. The close approach of Cys-41 to Cys-374 and Cys-41 to Cys-265, which is necessary for the cross-linking of these sites, appears incompatible with the models of F-actin structure [1,2]. However, model calculations reveal that the cross-linking results can be accommodated within these F-actin structures [1,2] by assuming dynamic behavior of loop 38–52, plug 262–274 and the C-terminus (unpublished). Dynamic properties were attributed to these structural elements in several previous studies [2,3,8,33]. It is notable also that the pyrene excimer and cross-linking results provide support for models of F-actin in which the hydrophobic plug extends over to the opposite actin strand and forms intermolecular contacts with loop 38–52 [1,2].

Earlier actin cross-linking studies [34] and the work on subtilisin-cleaved actin [9] suggested that structural flexibility and dynamic changes in F-actin may be necessary for its biological functions, and in particular for motion and force generation with myosin. The inhibition of the in vitro mobility of actin due to ANP cross-linking of loop 38–52 to the C-terminus on adjacent actins (Q41-C374) sheds light on the link between actin filament dynamics and function. Our results show that dynamic changes that occur at loop (38–52)/plug (262–274)/C-terminus interface in F-actin are important to its function. We may speculate that these changes need to be synchronized with myosin changes in the cross-bridge cycle to allow for the mechanochemical coupling in the actomyosin system. Our results also suggest a common denominator for the earlier observations on structural sensitivity and functional changes (in vitro motility) in F-actin depending on the modifications of loop 38–52 and the C-terminal region. As residues in these sites may interact with each other at the loop/plug/C-terminus interface, all such manipulations alter the interface and its dynamic properties.

In summary, the results of pyrene fluorescence and cross-linking experiments support the hypothesis that loop 38–52, hydrophobic plug 262–274 and the C-terminus cooperatively form an intermolecular interface in F-actin [21]. The interactions of these structural elements in F-actin can be accommodated within the existing models of F-actin structure with the provision for their considerable motion flexibility. The dynamic

properties and changes at the loop/plug/C-terminus interface are essential to the mechanochemical coupling in the actomyosin system.

Acknowledgements

This work was supported by USPHS Grant AR 22031 and NSF Grant MCB 9904599. We thank Drs. Masao Motoki and Katsuya Seguro for the gift of bacterial transglutaminase and Dr Gyorgy Hegyi for the gift of *N*-(4-azido-2-nitrophenyl) putrescine.

References

[1] K.C. Holmes, D. Popp, W. Gebhard, W. Kabsch, Atomic model of the actin filament, Nature 347 (1990) 44–49.
[2] M. Lorenz, D. Popp, K.C. Holmes, Refinement of the F-actin model against X-ray fiber diffraction data by the use of a directed mutation algorithm, J. Mol. Biol. 234 (1993) 826–836.
[3] M.M. Tirion, D. ben-Avraham, M. Lorenz, K.C. Holmes, Normal modes as refinement parameters for the F-actin model, Biophys. J. 68 (1995) 5–12.
[4] J. Hanson, Axial period of actin filaments, Nature 213 (1967) 353–356.
[5] A. McGough, B. Pope, W. Chiu, A. Weeds, Cofilin changes the twist of F-actin: implications for actin filament dynamics and cellular function, J. Cell Biol. 138 (1997) 771–781.
[6] A. Orlova, E.H. Egelman, Structural basis for the destabilization of F-actin by phosphate release following ATP hydrolysis, J. Mol. Biol. 227 (1992) 1043–1053.
[7] A. Orlova, E.H. Egelman, A conformational change in the actin subunit can change the flexibility of the actin filament, J. Mol. Biol. 232 (1993) 334–341.
[8] A. Orlova, E.H. Egelman, Structural dynamics of F-actin.1. Changes in the C-terminus, J. Mol. Biol. 245 (1995) 582–597.
[9] D.H. Schwyter, S.J. Kron, Y.Y. Toyoshima, J.A. Spudich, E. Reisler, Subtilisin cleavage of actin inhibits in vitro sliding movement of actin filaments over myosin, J. Cell Biol. 111 (1990) 465–470.
[10] S.Y. Khaitlina, J. Moraczewska, H. Strzelecka-Golaszewska, The actin/actin interactions involving the N-terminus of the DNase-I-binding loop are crucial for stabilization of the actin filament, Eur. J. Biochem. 218 (1993) 911–920.
[11] A. Muhlrad, P. Cheung, B.C. Phan, C. Miller, E. Reisler, Dynamic properties of actin — structural changes induced by beryllium fluoride, J. Biol. Chem. 269 (1994) 11852–11858.
[12] J.M. Squire, E.P. Morris, A new look at thin filament regulation in vertebrate skeletal muscle, Fed. Am. Soc. Exp. Biol. J. 12 (1998) 761–771.
[13] S.I. O'Donoghue, M. Miki, C.G. dos Remedios, Removing the 2 C-terminal residues of actin affects the filament structure, Arch. Biochem. Biophys. 293 (1992) 110–116.
[14] M. Mossakowska, J. Moraczewska, S. Khaitlina, H. Strzelecka-Golaszewska, Proteolytic removal of 3 C-terminal residues of actin alters the monomer-monomer interactions, Biochem. J. 289 (1993) 897–902.
[15] G. Drewes, H. Faulstich, Cooperative effects on filament stability in actin modified at the C-terminus by substitution or truncation, Eur. J. Biochem. 212 (1993) 247–253.
[16] R.H. Crosbie, C. Miller, P. Cheung, T. Goodnight, A. Muhlrad, E. Reisler, Structural connectivity in actin-Effect of C-terminal modifications on the properties of actin, Biophys. J. 67 (1994) 1957–1964.
[17] I. Kuznetsova, O. Antropova, K. Turoverov, S. Khaitlina, Conformational changes in subdomain I of actin induced by proteolytic cleavage within the DNase I-binding loop-energy transfer from tryptophan to AEDANS, FEBS Lett. 383 (1996) 105–108.
[18] E. Kim, E. Reisler, Intermolecular coupling between loop 38–52 and the C-terminus in actin filaments, Biophys. J. 71 (1996) 1914–1919.
[19] A. Orlova, E. Prochniewicz, E.H. Egelman, Cooperativity in structural transitions, J. Mol. Biol. 245 (1995) 598–607.
[20] A. Orlova, E.H. Egelman, Cooperative rigor binding of myosin to actin is a function of F-actin structure, J. Mol. Biol. 265 (1997) 469–474.
[21] C. Owen, D. DeRosier, A 13-A map of the actin-scruin filament from the limulus acrosomal process, J. Cell Biol. 123 (1993) 337–344.
[22] C.J. Miller, T.C. Doyle, E. Bobkova, D. Botstein, E. Reisler, Mutational analysis of the role of hydrophobic residues in the 338–348 helix on actin in actomyosin interactions, Biochemistry 35 (1996) 3670–3676.
[23] R.S.M. Sikorski, A. William, S. Tugendreich, P. Hieter, Allele shuffling: conjugational transfer, plasmid shuffling and suppressor analysis in *Saccharomyces cerevisiae*, Gene 155 (1995) 51–59.
[24] J.A. Spudich, S. Watt, The regulation of rabbit skeletal muscle contraction. I. Biochemical studies of the interaction of the tropomyosin-troponin complex with actin and the proteolytic fragments of myosin, J. Biol. Chem. 246 (1971) 4866–4871.
[25] D. Schwyter, M. Phillips, E. Reisler, Subtilisin-cleaved actin — polymerization and interaction with myosin subfragment-1, Biochemistry 28 (1989) 5889–5895.
[26] R.K. Cook, D. Root, C. Miller, E. Reisler, P.A. Rubenstein, Enhanced stimulation of myosin subfragment-1 ATPase activity by addition of negatively charged residues to the yeast actin NH_2 terminus, J. Biol. Chem. 268 (1993) 2410–2415.
[27] J.F. Du, C. Frieden, Kinetic studies on the effect of

yeast cofilin on yeast actin polymerization, Biochemistry 37 (1998) 13276–13284.
[28] L. Feng, E. Kim, W.L. Lee et al., Fluorescence probing of yeast actin subdomain 3/4 hydrophobic loop 262–274-Actin-actin and actin-myosin interactions in actin filaments, J. Biol. Chem. 272 (1997) 16829–16837.
[29] G. Hegyi, M. Mak, E. Kim, M. Elzinga, A. Muhlrad, E. Reisler, Intrastrand cross-linked actin between Gln-41 and Cys-374. I. Mapping of sites cross-linked in F-actin by N-(4-azido-2-nitrophenyl) putrescine, Biochemistry 37 (1998) 17784–17792.
[30] T. Kouyama, K. Mihashi, Fluorimetry study of N-(1-pyrenyl)iodoacetamide-labeled F-actin. Local structural change of actin protomer both on polymerization and on binding of heavy meromyosin, Eur. J. Biochem. 114 (1981) 33–38.
[31] S.S. Lehrer, Pyrene excimer fluorescence as a probe of protein conformational change, in: B.B. Biswas, S. Roy (Eds.), Subcellular Biochemistry, Proteins: Structure, Function, and Engineering, 24, Plenum Press, New York, 1995, pp. 115–131.
[32] E. Kim, E. Bobkova, C.J. Miller et al., Intrastrand cross-linked actin between Gln-41 and Cys-374. III. Inhibition of motion and force generation with myosin, Biochemistry 37 (1998) 17801–17809.
[33] M. Steinmetz, K. Goldie, U. Aebi, A correlative analysis of actin filament assembly, structure, and dynamics, J. Cell Biol. 138 (1997) 559–574.
[34] E. Prochniewicz, T. Yanagida, Inhibition of sliding movement of F-actin by cross-linking emphasizes the role of actin structure in the mechanism of motility, J. Mol. Biol. 216 (1990) 761–772.